

D 742754

R-925-ARPA

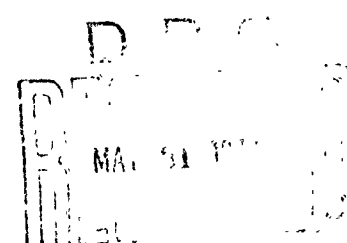
April 1972

Diffraction Patterns Produced by Focused Laser Beams

J. H. Rosen

A Report prepared for
ADVANCED RESEARCH PROJECTS AGENCY

Reproduced by
**NATIONAL TECHNICAL
INFORMATION SERVICE**
Springfield, Va 22151



Rand
SANTA MONICA, CA 90406

49

DOCUMENT CONTROL DATA

1. ORIGINATING ACTIVITY The Rand Corporation		2a. REPORT SECURITY CLASSIFICATION UNCLASSIFIED
		2b. GROUP
3. REPORT TITLE DIFFRACTION PATTERNS PRODUCED BY FOCUSED LASER BEAMS		
4. AUTHOR(S) (last name, first name, initial) Rosen, J. H.		
5. REPORT DATE April 1972	6a. TOTAL NO. OF PAGES 50	6b. NO. OF REFS. 15
7. CONTRACT OR GRANT NO. DAHC15 67 C 0141	8. ORIGINATOR'S REPORT NO. R-925-ARPA	
9a. AVAILABILITY/LIMITATION NOTICES DDC-A		9b. SPONSORING AGENCY Advanced Research Projects Agency
10. ABSTRACT Investigation of diffraction and jitter--two factors that influence the energy density produced by a laser beam projected from an aperture and focused onto a distant surface. The report first examines the characteristics of diffraction patterns produced by circular apertures with circular central obscurations and gaussian illuminations. Formulas, tables, and graphs are presented that enable the reader to estimate the peak intensity, the spot size, the power within the spot, and the average intensity over the spot that can be achieved by a given laser/telescope system. Attention is then directed to the problem of estimating energy densities when the center of the diffraction pattern jitters about an aim point on the target. A method is presented for estimating the effect of jitter that depends, in part, on approximating a real diffraction pattern with a gaussian pattern.		11. KEY WORDS Lasers Optics

Bibliographies of Selected Rand Publications

Rand maintains a number of special subject bibliographies containing abstracts of Rand publications in fields of wide current interest. The following bibliographies are available upon request:

*Aerodynamics • Arms Control • Civil Defense
Communication Satellites • Communication Systems
Communist China • Computer Simulation • Computing Technology
Decisionmaking • Game Theory • Maintenance
Middle East • Policy Sciences • Program Budgeting
SIMSCRIPT and Its Applications • Southeast Asia
Space Technology and Planning • Statistics • Systems Analysis
USSR/East Europe • Weapon Systems Acquisition
Weather Forecasting and Control*

To obtain copies of these bibliographies, and to receive information on how to obtain copies of individual publications, write to: Communications Department, Rand, 1700 Main Street, Santa Monica, California 90406.

PREFACE

During the past two and one-half years, The Rand Corporation has been conducting a study for the Advanced Research Projects Agency of possible new applications for lasers. Several reports have already resulted from this study, which is still in process. The results presented in these reports have depended, in part, on detailed calculations of the diffraction patterns produced by focused laser beams. These calculations, described herein, show relationships between characteristics of the beam as it leaves the output aperture and those of the beam when it reaches a focus on a distant surface.

Some of the general results given in this report have also appeared elsewhere in the literature. However, almost none of our detailed, specific results have been available until now. It was the need for these data in the larger study that prompted us to undertake these calculations. They are being published here so that they may be made widely available for use in the design of laser systems and in the analysis of their performance.

SUMMARY

Some types of lasers produce (ideally) a monochromatic collimated beam with a gaussian radial-intensity variation. The beam can be expanded by telescope-like optics, projected from an output aperture, focused onto a distant target, and kept aimed at the same point on the target for some appropriate time interval. The objective of this procedure is to achieve a high energy density.

This report examines two of the factors that influence the resultant energy density: diffraction, which prevents the beam from focusing to a point, and jitter of the diffraction pattern, which spreads energies over a larger area. Diffraction-pattern characteristics are found from numerical solutions of the Fraunhofer diffraction integral for circular apertures with circular central obscurations and gaussian illuminations. For describing intensity patterns, we have chosen the "spot" to be the circular area whose edge lies at the points where the intensity has fallen to one-half of the peak, central value. Formulas, tables, and graphs are presented that enable the reader to estimate the peak intensity, the spot size, the power within the spot, and the average intensity over the spot. Required inputs are the range, the radiated power, the aperture diameter, the wavelength, the fraction of the aperture area that is obscured, and a measure of the amount of truncation of the gaussian illumination.

The average intensities that result from a jittering beam are easily estimated if both the jitter statistics and the diffraction pattern are gaussian--the two combine (convolve) to yield another gaussian pattern. This report shows that the high-intensity portion of a diffraction pattern can be fitted closely with a gaussian pattern by choosing the gaussian parameters so as to match the size and power of the diffraction spot.

CONTENTS

PREFACE	iii
SUMMARY	v
SYMBOLS	ix
Section	
I. BACKGROUND AND OVERVIEW	1
II. DIFFRACTION PATTERNS	3
Inputs and Methodology	3
Results	13
III. ENERGY DENSITIES PRODUCED BY A JITTERING BEAM	26
A Method for Estimating the Time-Averaged Intensity	26
The Gaussian Approximation	28
Final Form of the Intensity Equation	35
REFERENCES	39

SYMBOLS

A = area within the aperture perimeter = $\pi D^2/4$

D = aperture diameter

F = obscuration fraction (the fraction (ϵ^2) of area A that is obscured)

f = fraction of power P in the focal plane contained within the half-intensity circle

$f(\beta)$ = fraction of power P in the focal plane contained within a circle of radius β

G = gaussian power-correction factor (GP is the total power in the gaussian approximation to a real diffraction pattern)

h = dimensionless angular radius of the half-intensity circle (unit angle = λ/D)

I = intensity (power per unit area) at a point in the focal plane

I_0 = maximum intensity (power per unit area) in the focal plane

J_0 = the zero-order Bessel function

m = diffraction limit (if θ is the spot diameter for a diffraction-limited system, $m\theta$ is the diameter for an " m times diffraction-limited" system)

n = taper parameter = $\frac{\text{aperture radius}}{\text{beam radius}} = \frac{D/2}{w}$

P = power radiated from the aperture to the focal plane (no transmission losses)

R = distance from the aperture to the focal plane

r = radial distance in the plane of the aperture (see Fig. 1)

s = dimensionless standard deviation of a gaussian approximation to a diffraction pattern [$\sigma_D = s(\lambda/D)R$]

t = time interval during which the laser beam stays focused on a target

U = wave amplitude at points in the focal plane ($I = |U|^2$)

u = wave amplitude at points in the plane of the aperture

$w = 1/e^2$ radius of a gaussian beam incident on the aperture

$w_0 = 1/e^2$ radius of a gaussian beam at the focal plane ($w_0 = 2\sigma_D$)

z = dimensionless variable of integration denoting radial distance in the aperture plane = $2r/D$

α = radial angle subtended by a radial distance ρ in the focal plane when viewed from the aperture = ρ/R (see Fig. 1)

α_D = angular standard deviation associated with a circular gaussian diffraction pattern = σ_D/R

α_J = angular standard deviation associated with a circular gaussian probability density function = σ_J/R

β = dimensionless radial angle = $\frac{\alpha}{\lambda/D}$ (see Fig. 1 for α)

ϵ = obscuration ratio (the ratio of the diameter of the central obscuration to the diameter of the aperture) = \sqrt{F}

λ = wavelength

ρ = radial distance in the focal plane (see Fig. 1)

σ = standard deviation of the two normal distributions that combine to form the circular gaussian distribution

σ_D = linear standard deviation associated with a circular gaussian diffraction pattern

σ_J = linear standard deviation associated with a circular gaussian probability-density function (jitter)

$\phi(\beta)$ = dimensionless intensity at a radial angle β in the focal plane; unit intensity = PA/λ^2R^2

$\overline{\phi(\beta)}$ = dimensionless intensity averaged over a disc of radius β in the focal plane

ϕ_0 = maximum dimensionless intensity in the focal plane

$\overline{\phi}$ = dimensionless intensity averaged over the half-intensity disc in the focal plane

I. BACKGROUND AND OVERVIEW

Some types of lasers produce (ideally) a monochromatic collimated beam with a gaussian radial-intensity variation.⁽¹⁾ This beam can be expanded by telescope-like optics, projected from an output aperture, focused onto a distant target, and kept aimed at that point on the target for some appropriate time interval. The focusing produces a high power density by concentrating most of the projected power onto a small spot on the target. Keeping the location of the spot fixed produces a high energy density.

For high-quality optics, one of the factors that determines how much concentration of power is possible is diffraction. Section II of this report examines the characteristics of diffraction patterns produced by circular apertures with circular central obscurations. Special emphasis is placed on the effects of truncation and obscuration. A few of the patterns are described in considerable detail; i.e., intensity and included power are given as a function of radial distance in the focal plane. For more concise pattern descriptions we have chosen the "spot" to be the circular area whose edge lies at the points where the intensity has fallen to one-half of the peak, central value. Formulas, tables, and graphs are presented that enable the reader to estimate the peak intensity, the spot size, the power within the spot, and the average intensity over the spot that can be achieved by a given laser/telescope system.

If the diffraction pattern stays fixed with respect to the target surface, the resultant energy densities are easily determined by multiplying the power densities by the time interval. Section III addresses the problem of estimating energy densities when the center of the diffraction pattern moves or "jitters" about an aim point on the target. A method for estimating the effect of jitter is presented that depends, in part, on approximating a real diffraction pattern with a gaussian pattern. Adequate approximations can be constructed by using some of the pattern characteristics developed in Section II.

Some of the general results given in this report have also appeared elsewhere in the literature. Many of the references listed at

the end of this report include studies of the effects of truncation and, to a lesser extent, obscuration on the propagation of gaussian beams. But they do not contain the detailed, specific values for the half-intensity spot sizes and included powers that are given in this report. It was this lack of data that prompted us to undertake the calculations reported here.

II. DIFFRACTION PATTERNS

This section presents characteristics of diffraction patterns (or "images") produced by circular apertures with circular central obscurations. The radiation incident upon the aperture is assumed to be a monochromatic beam with a converging spherical wave front and a gaussian radial-intensity* variation. The wave front leaving the aperture will be truncated and sometimes obscured. We will compute the diffraction pattern that occurs in the geometric focal plane, i.e., in a plane that is normal to the beam axis and located at the center of curvature of the emerging wave front. Results of such computations are often called "far-field" results because they also describe the radiation pattern at great distances from apertures illuminated by plane waves. All are examples of Fraunhofer diffraction.

INPUTS AND METHODOLOGY

The emerging beam is centered in the aperture. Figure 1 shows the geometry and identifies some of the parameters: D is the aperture

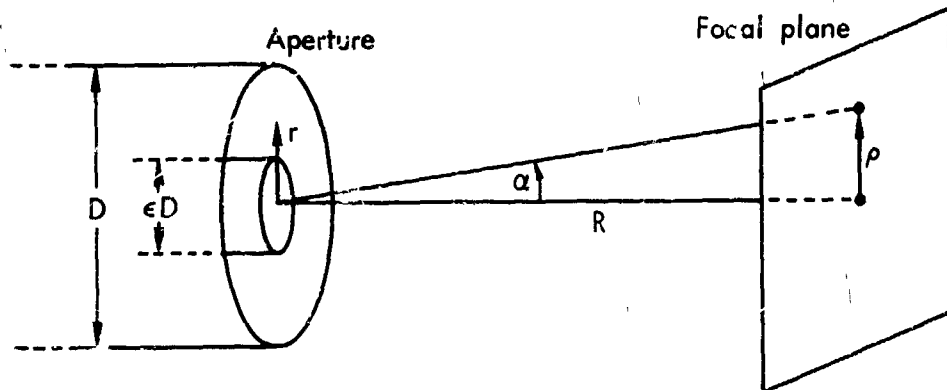


Fig. 1—The geometry and the coordinates

* Throughout this report, intensity refers to power per unit area. (In the current literature, this quantity is often called irradiance.)

diameter, ϵD is the diameter of the obscuration,^{*} and R is the distance to the focal plane. Because of the axial symmetry of the output radiation, the diffraction pattern will have the same kind of symmetry. Points in the focal plane are denoted either by their radial distance ρ from the center of the pattern or by the "radial" angle α that ρ subtends when viewed from the aperture.

Points in the aperture plane are denoted by their radial distance r from the center. The gaussian amplitude distribution of the aperture illumination can be expressed as

$$u(r) = u_0 \exp(-r^2/w^2) \quad (1)$$

where w is a constant defined to be the beam "radius." The intensity is given by $|u|^2$. Thus w is the radial distance at which the intensity has fallen to $1/e^2$ of its axial value.

Note that Eq. (1) describes the amplitude of a *plane* wave. If it became necessary to specify the wave-front curvature, $u(r)$ would be multiplied by a complex phase factor of the form $\exp(-i\pi r^2/\lambda R)$. However, Eq. (1) is the proper amplitude expression to use in the equations that will be presented later.

Solution for an Infinite Gaussian Beam

An analytical solution exists for the wave propagation of an ideal (infinite) beam.⁽²⁾ Dickson⁽³⁾ and Bloom⁽⁴⁾ have estimated that if the aperture radius is at least twice as large as the beam radius, the effects of the truncation are "negligible" and the analytical solution is adequate. For this idealized case, the beam remains gaussian everywhere. The diffraction pattern at the focal plane has a radius w_0 given by⁽³⁾

$$w_0 = \frac{\lambda R}{\pi w}$$

^{*}The quantity ϵ , which is the ratio of the two diameters ϵD and D , is usually called the *obscuration ratio*.

where λ is the wavelength. The focal-plane intensity distribution $I(\rho)$ is then

$$I(\rho) = I_0 \exp(-2\rho^2/w_0^2) \quad (2)$$

The intensity I_0 at the center of the pattern can be found by equating the total incident power P to the integral of $I(\rho)$ over the focal plane. The resultant value of I_0 is

$$I_0 = \frac{2P}{\pi w_0^2} = 2 \frac{P \pi w_0^2}{\lambda^2 R^2} \quad (3)$$

The Diffraction Equation

When the output beam is significantly truncated or obscured, the diffraction pattern is no longer gaussian; rather, it resembles an Airy pattern, i.e., a bright central disc surrounded by alternate dark and light rings. To find the intensity at a point in the focal plane, we must evaluate the Fraunhofer diffraction integral which yields the wave amplitude $U(\rho)$.* The intensity I is then given by $I = |U|^2$.

For a uniformly illuminated circular aperture with a central obscuration, the Fraunhofer diffraction integral is⁽⁵⁾

$$U(\alpha) = \frac{2\pi}{\lambda R} u \int_{-\frac{D}{2}}^{\frac{D}{2}} J_0\left(\frac{2\pi}{\lambda} \alpha r\right) r dr$$

where u is the uniform wave amplitude at the aperture, and J_0 is the zero-order Bessel function. Note that the integration is performed

* To amplify an earlier comment, Fraunhofer diffraction applies either in a focal plane or in the far field ($R \gg \lambda^2/\lambda$) of a collimated beam.⁽⁵⁾ Elsewhere, the Fresnel diffraction integral must be used. Results for such "near-field" intensities produced by truncated gaussian apertures are presented in Refs. 6 and 7.

over the illuminated portion of the aperture and that the radial angle α is being used to denote the radial location of the point in the diffraction pattern.*

If the aperture illumination is nonuniform, the amplitude $u(r)$ must be brought under the integral sign. For a gaussian illumination, the result is

$$U(\alpha) = \frac{2\pi}{\lambda R} u_0 \int_{\epsilon \frac{D}{2}}^{\frac{D}{2}} \exp(-r^2/w^2) J_0 \left(\frac{2\pi}{\lambda} \alpha r \right) r \, dr \quad (4)$$

The diffraction equation (Eq. (4)) can be cast in a form that is more suitable for calculating and presenting results. First, we introduce two key aperture parameters, n and F , that specify the amount of truncation and obscuration. They are defined as

$$n = \frac{\text{aperture radius}}{\text{beam radius}} = \frac{D/2}{w}$$

F = the fraction of the total circular aperture area ($\pi D^2/4$) that is obscured = ϵ^2

(These parameters will be discussed in more detail later.) Next, we introduce the dimensionless radial angle $\beta = \frac{\alpha}{\lambda/D}$ and change the variable of integration to $z = 2r/D$. As a result of these four changes, the diffraction equation will become

$$U(\beta) = \frac{2\lambda}{\lambda R} u_0 \int_{\frac{1}{F}}^1 e^{-\pi n^2 z^2} J_0(\pi \beta z) z \, dz$$

where A is the full circular area $\pi D^2/4$.

* The approximation $\epsilon = \pi R$ is used here and elsewhere throughout this report.

Finally, we find an expression for u_0 by equating the total radiated power P to the integral of the intensity over the aperture. That is,

$$\begin{aligned}
 P &= 2\pi \int_{-\frac{D}{2}}^{\frac{D}{2}} u_0^2 e^{-2n^2 z^2} r dr \\
 &= 2Au_0^2 \int_{-\frac{D}{2}}^{\frac{D}{2}} e^{-2n^2 z^2} z dz \\
 &= \frac{Au_0^2}{2n} (e^{-2Fn^2} - e^{-2n^2})
 \end{aligned}$$

Thus

$$u_0 = \left(\frac{2P}{A}\right)^{\frac{1}{2}} \frac{n}{\left(e^{-2Fn^2} - e^{-2n^2}\right)^{\frac{1}{2}}}$$

so the diffraction equation becomes

$$u(\beta) = \left(\frac{PA}{\lambda^2 R^2}\right)^{\frac{1}{2}} \frac{2\sqrt{2}n}{\left(e^{-2Fn^2} - e^{-2n^2}\right)^{\frac{1}{2}}} \int_{-\frac{D}{2}}^{\frac{D}{2}} e^{-n^2 z^2} J_0(\pi\beta z) z dz \quad (5)$$

An advantage of this formulation is that all of the parameters that have physical dimensions have disappeared from the integral and appear together in the single expression $PA/\lambda^2 R^2$. This quantity is of special importance in diffraction theory because it is the expression

for the maximum intensity in the Fraunhofer diffraction pattern produced by a uniformly illuminated aperture of area A .* It is a natural choice for a normalizing factor, i.e., a unit of intensity. Therefore, the final statement of the diffraction formula is as follows: We define a dimensionless intensity $\phi(\beta)$ by the expression

$$\phi(\beta) = \left[\frac{2\sqrt{2n}}{\left(e^{-2Fn^2} - e^{-2n^2} \right)^{\frac{1}{2}}} \cdot \int_{\sqrt{F}}^1 e^{-n^2 z^2} J_0(\pi\beta z) z dz \right]^2 \quad (6)$$

and use $\phi(\beta)$ for describing the diffraction-pattern characteristics. The "physical" intensity can always be found later from

$$I(\beta) = \phi(\beta) \cdot \frac{PA}{\lambda^2 R^2} \quad (7)$$

and linear radii in the focal plane can always be found from $\alpha = \beta(\lambda/D)$ and $\rho = \alpha R$.

The Maximum Intensity

The maximum intensity occurs at the center of the image, which corresponds to $\beta = 0$. When $\beta = 0$, the function $J_0 = 1$. This simplification of the integrand allows the diffraction integral to be evaluated in closed form. The resulting expression for the dimensionless maximum intensity ϕ_0 is**

$$\phi_0 = \frac{2}{n^2} \frac{e^{n^2(1-F)} - 1}{e^{n^2(1-F)} + 1} \quad (8)$$

* It is also the maximum possible intensity. Any nonuniformity of the aperture illumination will reduce the maximum. (8)

** Reference 9 presents a closed-form solution for the on-axis intensity for all ranges, including the focal range.

It is not difficult to verify that

$$\lim_{n \rightarrow 0} \phi_0 = 1 - F$$

This is a necessary result because $n \rightarrow 0$ implies a uniform aperture illumination. In that case we must have

$$I_0 = \frac{PA'}{\lambda^2 R^2}$$

where $A' = A(1 - F)$ is the true aperture area.

Equations for Included Power and Average Intensity

Other important diffraction-pattern characteristics, aside from $\phi(\beta)$ itself, are $f(\beta)$, the fraction of the total power in the focal plane contained within a circle of radius β ; and $\bar{\phi}(\beta)$, the average intensity over a circle (or "disc") of radius β . Starting with

$$f(\beta) = \frac{1}{P} \int_0^{\beta} \frac{PA}{\lambda^2 R^2} \phi(\beta) 2\pi \beta d\beta$$

and using the relation $\beta = \beta(z/D)R$, we obtain

$$f(z) = \frac{\pi^2}{2} \int_0^z \phi(z) z dz \quad (9)$$

To find a useful expression for $\bar{\phi}(z)$, we start with the required relationship

$$\bar{\phi}(z) = \frac{PA}{\lambda^2 R^2} = \frac{f(z) + P}{z^2}$$

and obtain

$$\overline{\phi(\beta)} = \frac{4}{\pi^2 \beta^2} f(\beta) \quad (10)$$

Selected Input Values for n and F

The equation for $\phi(\beta)$ shows that for a given value of β , the intensity ϕ depends upon the values of only two parameters, n and F . As defined earlier, $\beta = (D/2)/w$. The introduction of n allows the aperture-illumination amplitude to be written as $u = u_0 \exp[-n^2(2r/D)^2]$. At the edge of the aperture the intensity falls to $\exp(-2n^2)$ of its axial value. Figure 2 shows how the intensity varies across the aperture for $n = 0, 0.5, 1.0, 1.5$, and 2.0 . These five illuminations encompass a very wide range. Note that $n = 0$ implies a uniform illumination.* The greater the value of n , the more steeply the intensity curve tapers from the center to the edge. Therefore we shall call n the "taper" parameter in the remainder of this discussion. This parameter is a measure of the nonuniformity of the illumination.

The obscuration fraction F is the fraction of the total area A that is obscured. Figure 3 shows the aperture appearances for $F = 0, 0.1, 0.2, 0.3, 0.4$, and 0.5 . Clearly, they encompass a wide range of obscurations.

Later in this section (pp. 13 - 19), certain specific and aggregate characteristics of diffraction patterns will be presented for all combinations of n and F .

Proper Interpretation of P and A

Before we present results, some words of caution are appropriate. It is important to remember that the power P in the expression $PA/\lambda^2 R^2$ is the power radiated from the aperture (to be even more precise, P

* By having earlier factored P and D out of the diffraction equation, we have avoided the implication that no power is radiated if $n = 0$.

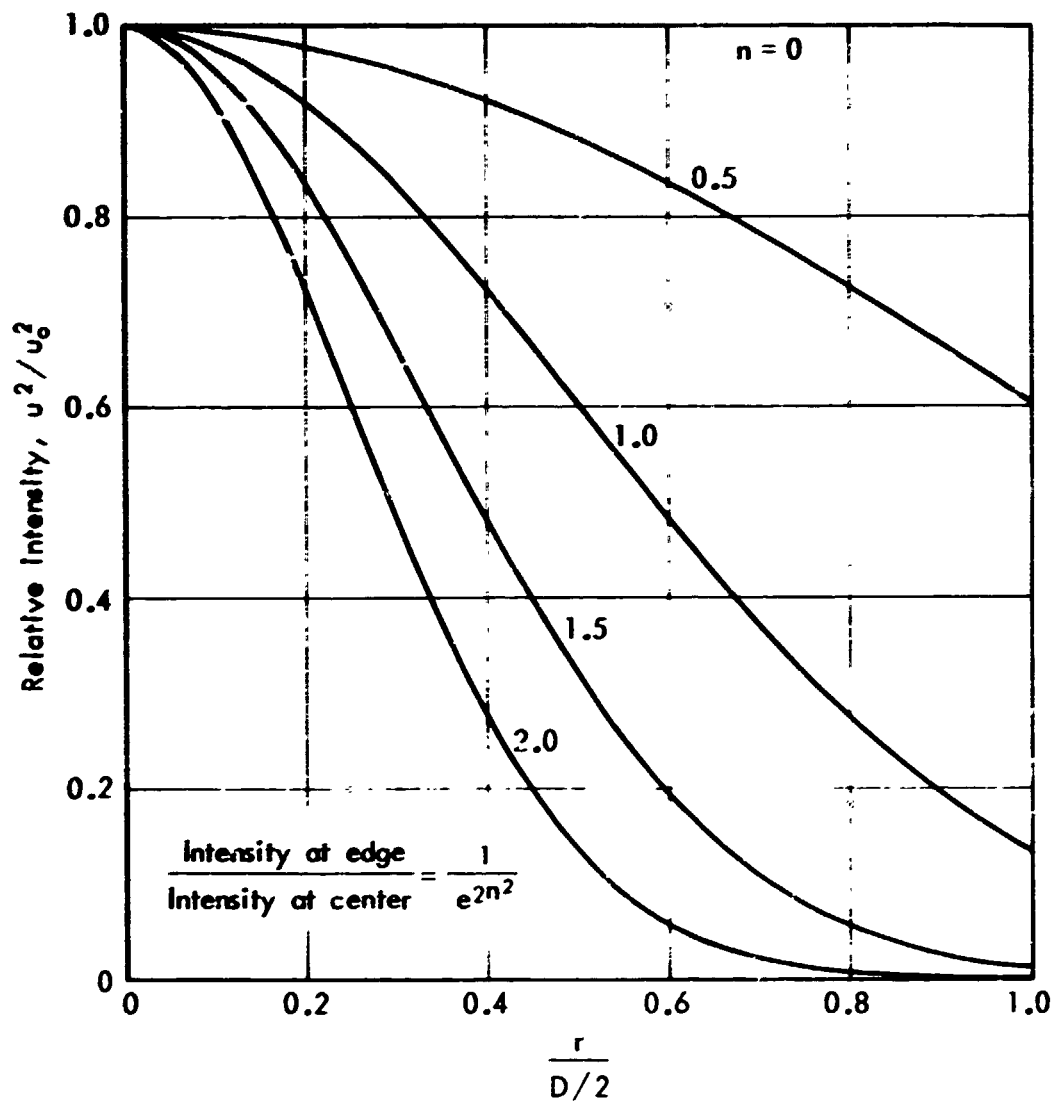


Fig. 2—Aperture intensity distribution

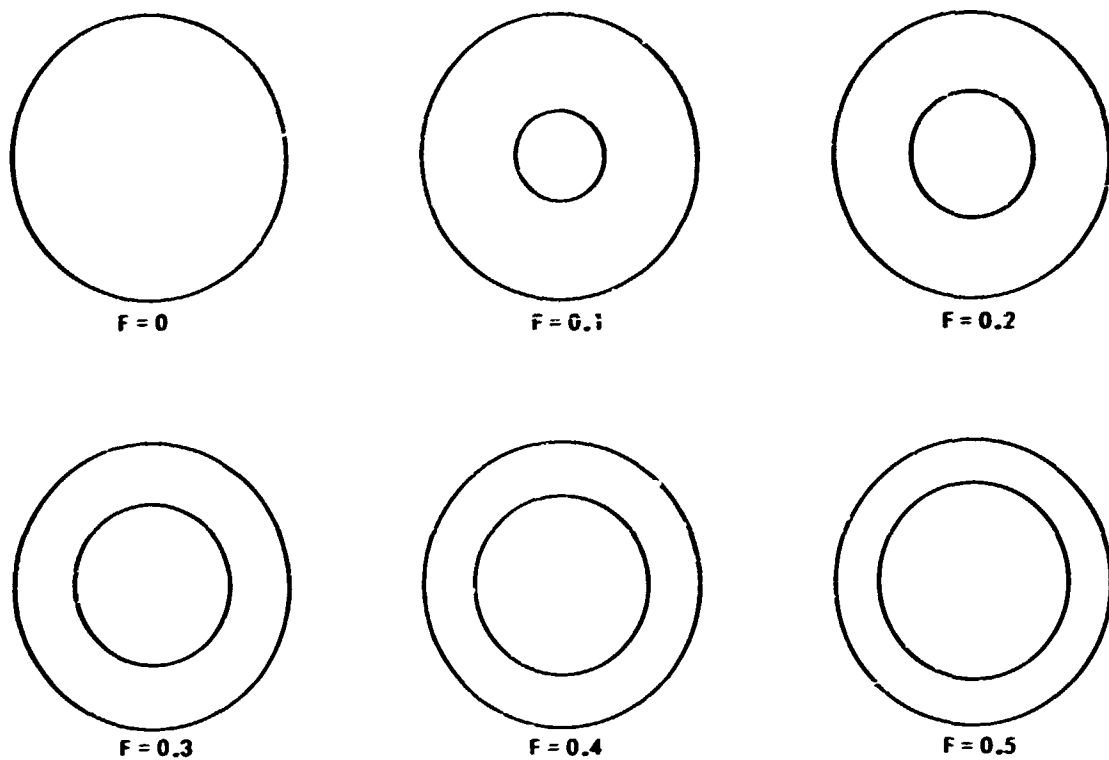


Fig. 3—Aperture appearances for various obscuration fractions, F

should be the power that reaches the focal plane, but we will assume no transmission losses). The power of the laser beam that enters the beam-expansion optics is not necessarily the same. To formulate the diffraction equations, we postulated that the wave is an ideal gaussian before it is truncated and obscured by the aperture. For such a case, it is easy to show that if the power of the ideal beam were P' , then the power transmitted by the aperture would be

$$P = P' \cdot (e^{-2Fn^2} - e^{-2n^2}) \quad (11)$$

the losses being caused by truncation and obscuration. But a real beam-expander might not work this way. This study has not examined methods for estimating such losses.

A second point to reemphasize is that the area A in the expression $PA/\lambda^2 R^2$ is not necessarily the illuminated area of the aperture. It is always equal to the full circular area $\pi D^2/4$. When there is obscuration, the illuminated area is equal to $A(1 - F)$.

RESULTS

First we will present, in detail, the patterns corresponding to a selected set of four pairs of values for n and F . Less detailed results will then be presented for the 30 pairs considered.

Detailed Diffraction-Pattern Characteristics

Figures 4 through 6 show intensity ϕ versus radial angle β for a selected set of tapers and obscurations. The tapers are $n = 0$, corresponding to uniform illumination, and $n = 1$, corresponding to a gaussian truncated at the $1/e^2$ radius. The obscurations are none ($F = 0$), and 10 percent ($F = 0.1$). The results in Figs. 4 through 6 were obtained by direct numerical integration of the diffraction integral. No general closed-form solution exists.* However, series solutions that may converge rapidly have been devised.^(7,10)

Figure 4 shows that tapering the illumination decreases the maximum intensity, widens the central disc, and reduces the intensity of the rings. Figures 5 and 6 show that obscuration decreases the maximum intensity, narrows the central disc, and increases the intensity of the first ring.

Figure 7 displays the fraction of the total power in the image

* For uniform illumination ($n = 0$), $\phi(\beta)$ can be found analytically.⁽⁵⁾ The solution, first found by Airy, is

$$\phi(\beta) = \frac{1}{1 - F} \left[\frac{2J_1(\pi\beta)}{\pi\beta} - F \frac{2J_1(\epsilon\pi\beta)}{\epsilon\pi\beta} \right]^2$$

where J_1 is the first-order Bessel function. Results obtained from this formula and from the analytical formula for ϕ , were compared with results obtained by numerical integration to assess the accuracy of the numerical methods. For all comparisons, quantities agreed to within at least three significant figures.

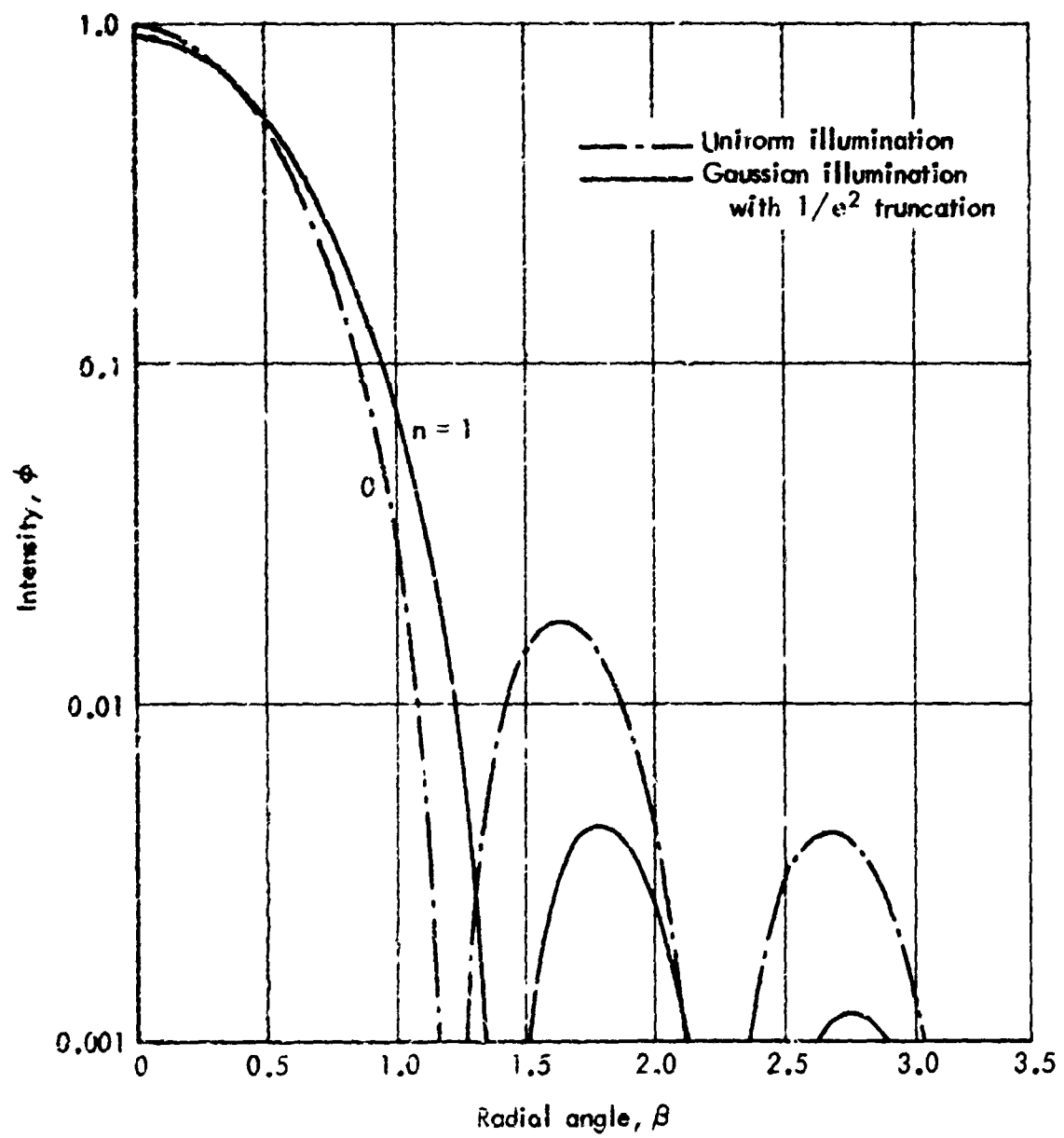


Fig. 4—Diffraction patterns for $F=0$ (no obscuration)

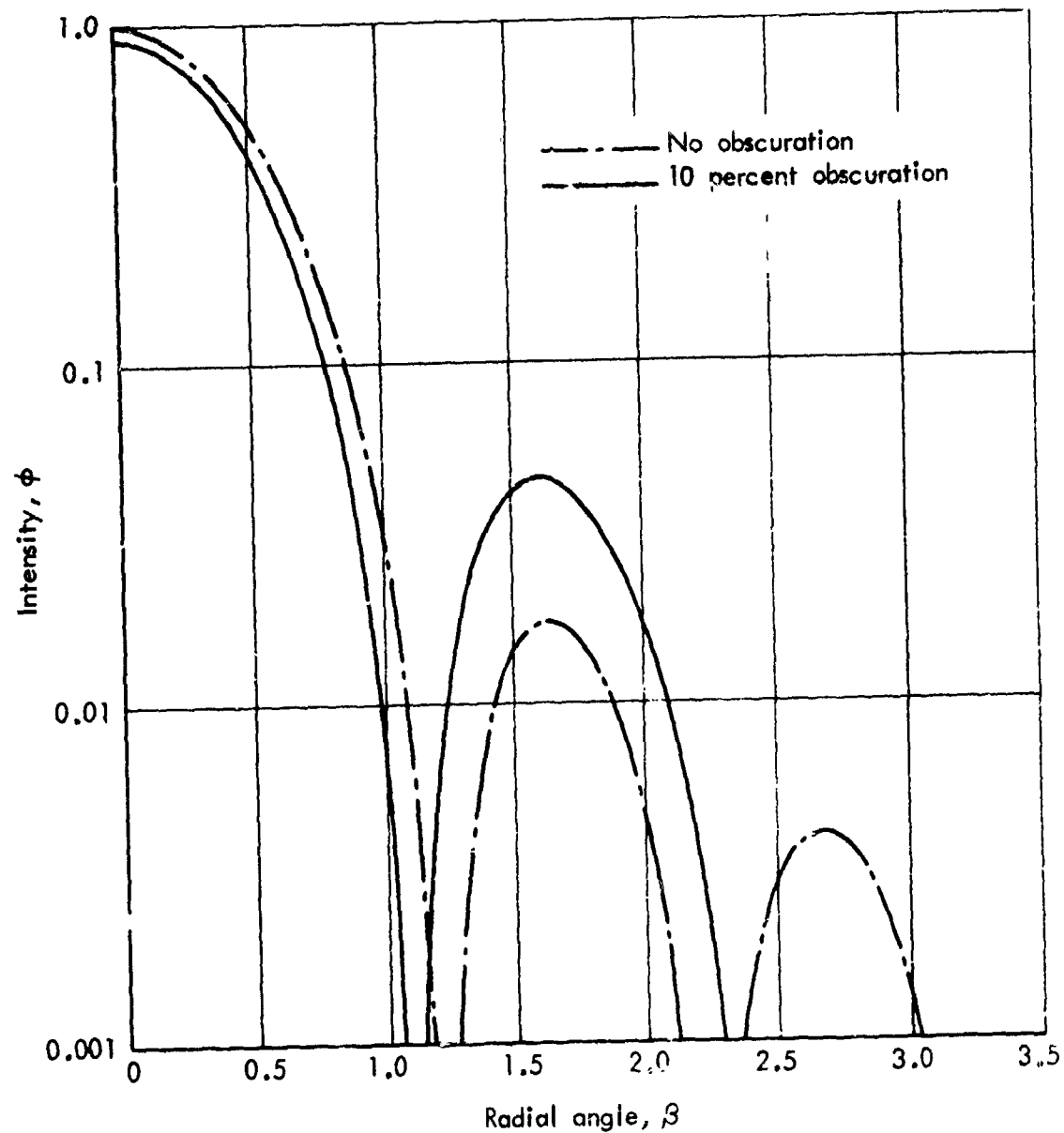


Fig. 5—Diffraction patterns for $n=0$ (uniform illumination)

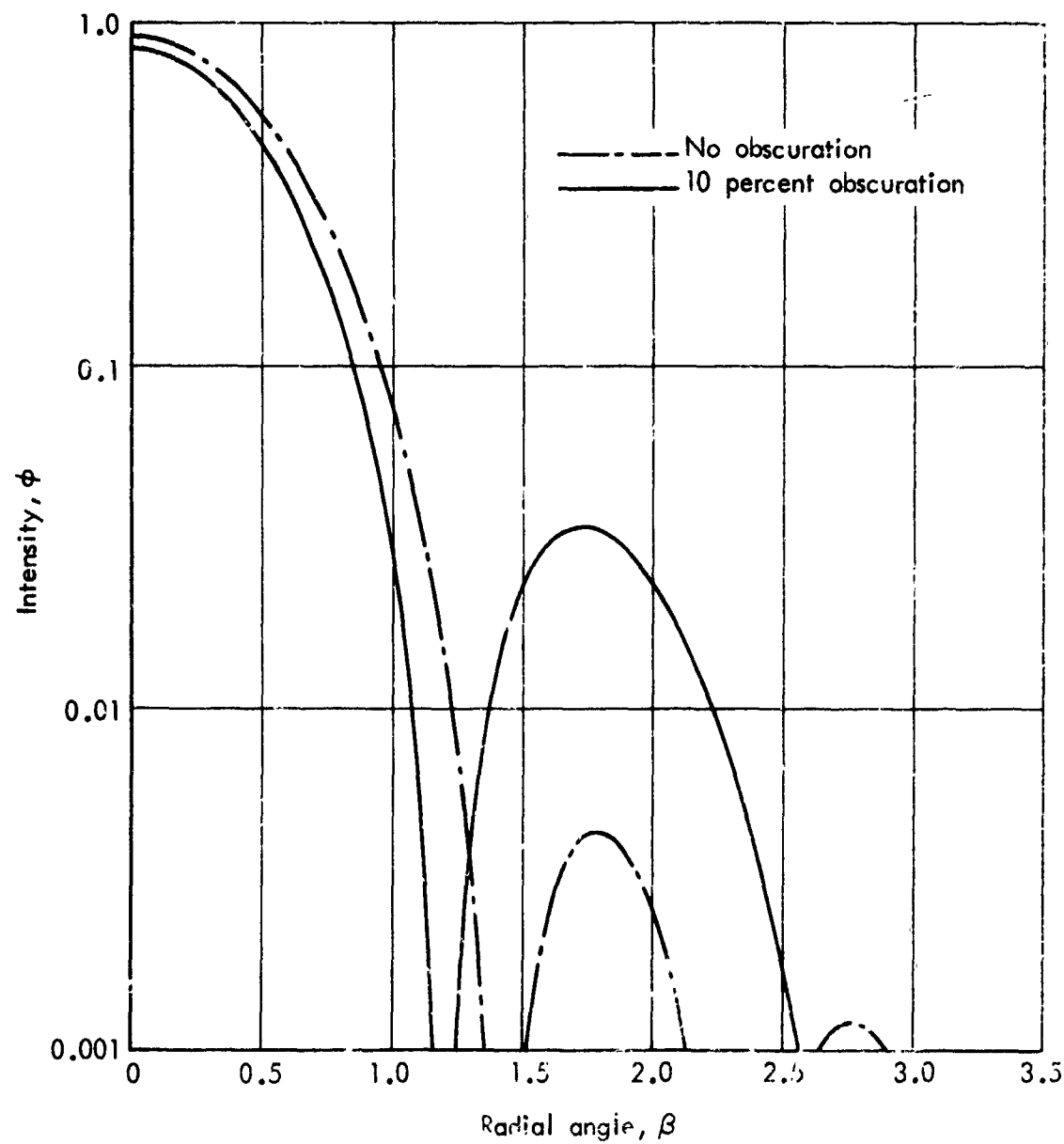


Fig. 6—Diffraction patterns for $n=1/2$ gaussian illumination with $1/e^2$ truncation)

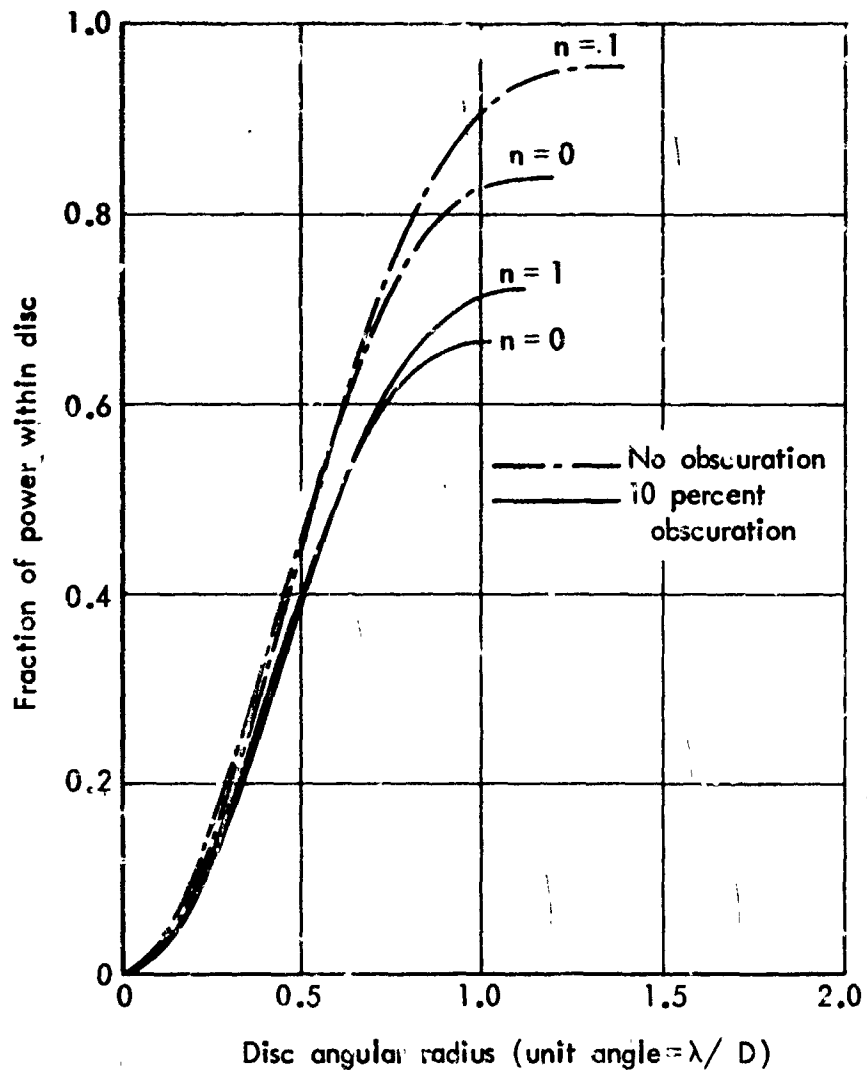


Fig.7—Fraction of image power within disc

that lies within circles (i.e., discs) of various radii. The curves show the behavior of the central portion of the pattern; they have been stopped at the first null. If they were extended farther, they would resemble step functions as successive rings are included within the circle. These curves illustrate the main effect of a central obscuration: It diffracts power into the rings.

Figure 8 displays the average intensity as a function of the size of the disc over which the average is taken. In laser-application studies, an average intensity is often used to describe the diffraction

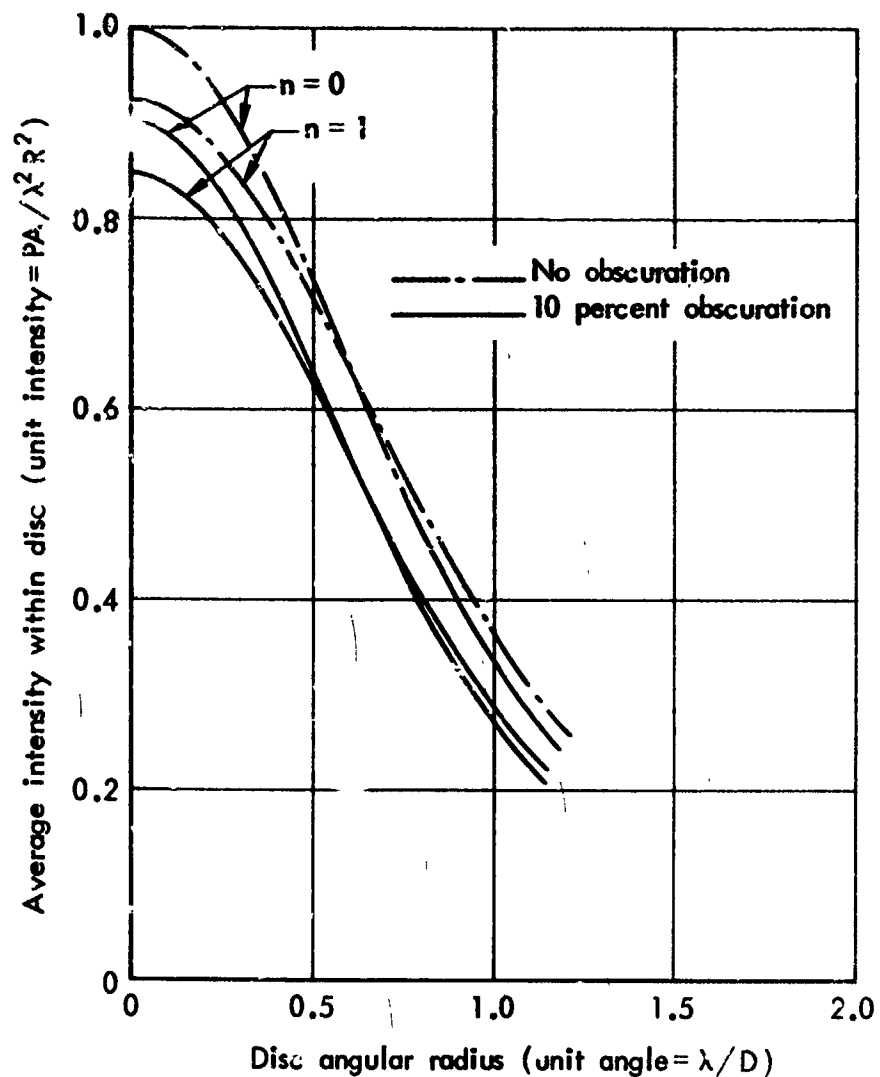


Fig. 8—Average intensities within disc

pattern, yet there is no agreement among investigators about what disc size should be chosen for taking the average. Figure 8 shows that the average intensity can be a strong function of this choice.

Table 1 summarizes some of the major characteristics of the central portions of these four patterns. The full central disc, the " $1/e^2$ " disc, and the "half-intensity" disc are considered. The radii of the latter two extend to the points where the intensity has fallen, respectively, to $1/e^2$ and one-half of the peak value.

Table 1
DIFFRACTION-PATTERN CHARACTERISTICS

Characteristic	Value			
	Uniform Illumination		Gaussian Illumination with $1/e^2$ Truncation	
	No Obscu- ration	10% Obscu- ration	No Obscu- ration	10% Obscu- ration
Peak intensity ^a	1.000	0.900	0.924	0.844
Full Central Disc				
Angular radius ^b	1.22	1.13	1.43	1.20
Power fraction	0.838	0.668	0.955	0.720
Average intensity	0.229	0.220	0.191	0.203
$1/e^2$ Disc				
Angular radius	0.823	0.773	0.915	0.830
Power fraction	0.767	0.615	0.866	0.663
Average intensity	0.459	0.417	0.419	0.390
Half-Intensity Disc				
Angular radius	0.514	0.498	0.566	0.522
Power fraction	0.475	0.385	0.530	0.412
Average intensity	0.727	0.655	0.671	0.613

^aUnit intensity = $PA/\lambda^2 R^2$.

^bUnit angle = λ/D .

Results for the Half-Intensity Disc

The maximum intensity ϕ_0 is an important descriptor of a diffraction pattern, but because it describes the power density at a single point, it gives no information about how much power can be concentrated into some finite-sized spot. For the following presentation of results we have chosen the half-intensity disc as the spot to be described.

Table 2 shows the values of the maximum intensity ϕ_0 for all combinations of the taper parameter n and the obscuration function F . In similar fashion, Tables 3 through 5 display the radii of the half-intensity discs (denoted by h), the power fraction within them (denoted by f), and their average intensities (denoted by $\bar{\phi}$).*

*Although three quantities are presented for the half-intensity disc, only two are independent. The three must satisfy the relationship $\phi_0 = 4f/\pi^2 h^2$.

Table 2

MAXIMUM INTENSITY^a

Obscuration Fraction, F	Maximum Intensity, ϕ_0				
	Taper Parameter, n				
	0.0	0.5	1.0	1.5	2.0
0.00	1.000	0.995	0.924	0.719	0.482
0.10	0.900	0.896	0.844	0.682	0.473
0.20	0.800	0.797	0.760	0.637	0.461
0.30	0.700	0.698	0.673	0.584	0.443
0.40	0.600	0.599	0.583	0.523	0.417
0.50	0.500	0.499	0.490	0.453	0.381

^aUnit intensity = $PA/\lambda^2 R^2$.

Table 3

HALF-INTENSITY RADIAL ANGLE^a

Obscuration Fraction, F	Half-Intensity Radial Angle, h				
	Taper Parameter, n				
	0.0	0.5	1.0	1.5	2.0
0.00	0.514	0.526	0.566	0.646	0.773
0.10	0.488	0.496	0.522	0.571	0.639
0.20	0.466	0.471	0.484	0.519	0.561
0.30	0.446	0.450	0.461	0.481	0.507
0.40	0.430	0.432	0.439	0.451	0.468
0.50	0.415	0.416	0.421	0.428	0.438

^aUnit angle = λ/D .

Table 4

FRACTION OF IMAGE POWER WITHIN THE HALF-INTENSITY CIRCLE

Obscuration Fraction, F	Fraction of Image Power, f				
	Taper Parameter, n				
	0.0	0.5	1.0	1.5	2.0
0.00	0.475	0.494	0.530	0.536	0.514
0.10	0.385	0.396	0.412	0.398	0.347
0.20	0.312	0.318	0.325	0.307	0.260
0.30	0.251	0.254	0.257	0.243	0.205
0.40	0.199	0.201	0.202	0.191	0.164
0.50	0.155	0.155	0.156	0.149	0.132

Table 5

AVERAGE INTENSITY WITHIN THE HALF-INTENSITY CIRCLE^a

Obscuration Fraction, F	Average Intensity, \bar{I}				
	Taper Parameter, n				
	0.0	0.5	1.0	1.5	2.0
0.00	0.727	0.722	0.671	0.521	0.349
0.10	0.655	0.652	0.613	0.493	0.344
0.20	0.582	0.580	0.553	0.463	0.335
0.30	0.510	0.509	0.490	0.425	0.322
0.40	0.437	0.436	0.425	0.381	0.304
0.50	0.364	0.364	0.357	0.330	0.278

^aUnit intensity = $PA/\lambda^2 R^2$.

To display the trends and to facilitate interpolation, we have presented these results graphically in Figs. 9 through 12.

As an illustration of how these general results can be applied to a specific case, consider a hypothetical system that radiates 30 kW of continuous-wave power at a wavelength of 10.6μ from an aperture 30 cm in diameter. (These parameters are consistent with the performance of CO_2 gas-dynamic lasers reported in Ref. 11.) We wish to compute the diffraction-pattern characteristics, using the half-intensity disc, when the beam is focused at a range of 500 m. First, we compute the unit intensity, $\text{PA}/\lambda^2 R^2$, as $7,550 \text{ w/cm}^2$. In this example, we assume that the aperture illumination is gaussian with $1/e^2$ truncation and 10 percent of the aperture area is obscured ($n = 1$, $F = 0.1$). Then, using the appropriate numbers from either the fourth column of Table 1 or from Tables 2 through 4, we find

$$\text{Peak intensity} = 0.844 (7,550) = 6,370 \text{ w/cm}^2$$

$$\text{Average intensity} = 0.613 (7,550) = 4,630 \text{ w/cm}^2$$

The radius of the spot of interest is $0.522 (\lambda/D)R$, which yields a spot diameter of 1.84 cm, about the size of a dime. The power within the spot is $0.412 P = 12.36 \text{ kW}$. It is easy to verify that this power divided by the spot area (2.67 cm^2) yields the average intensity computed above.

It must be remembered that the power densities computed by this method are theoretical upper limits. However, to illustrate the effect of such a high power density, if the target were indeed a silver dime and if it absorbed 10 percent of the incident radiation, it would melt in less than a second. (The reader is cautioned that melting silver dimes with laser beams is neither cost-effective nor legal.)

An Empirical Relationship Between Maximum and Average Intensities

When the taper and the obscuration vary, the maximum intensity ϕ_o and the average intensity $\bar{\phi}$ each vary over a wide range. However, the ratio $\bar{\phi}/\phi_o$ is very nearly a constant. We computed this ratio ($\bar{\phi}$ from

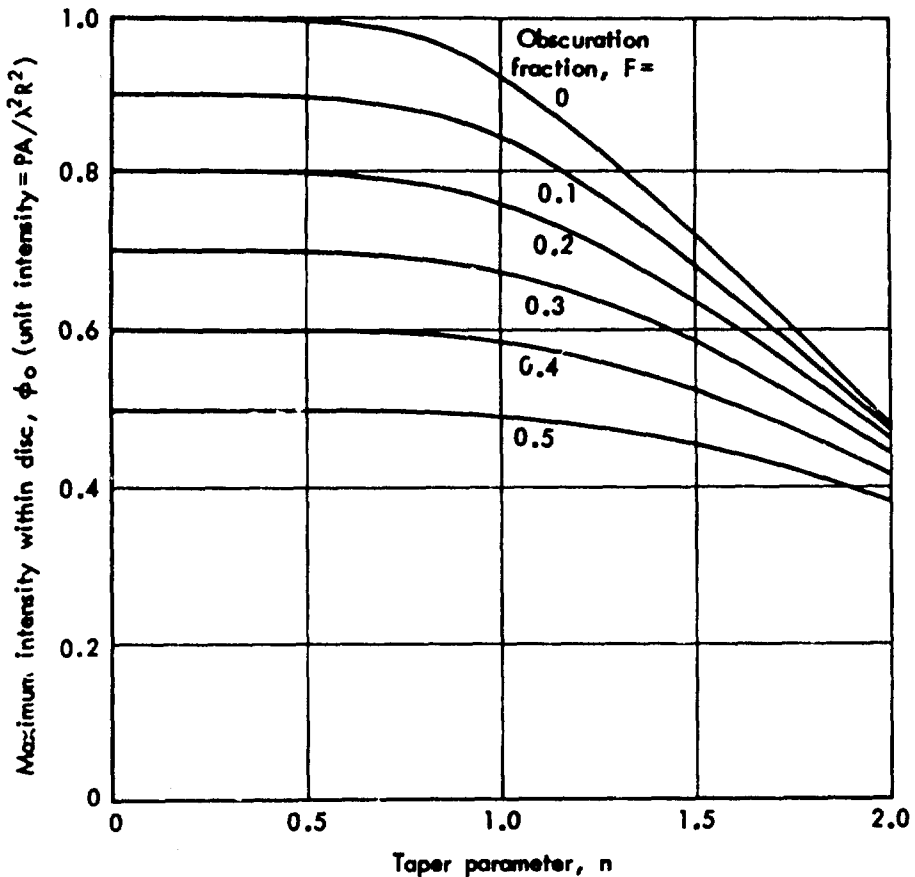


Fig. 9—Maximum intensity within disc

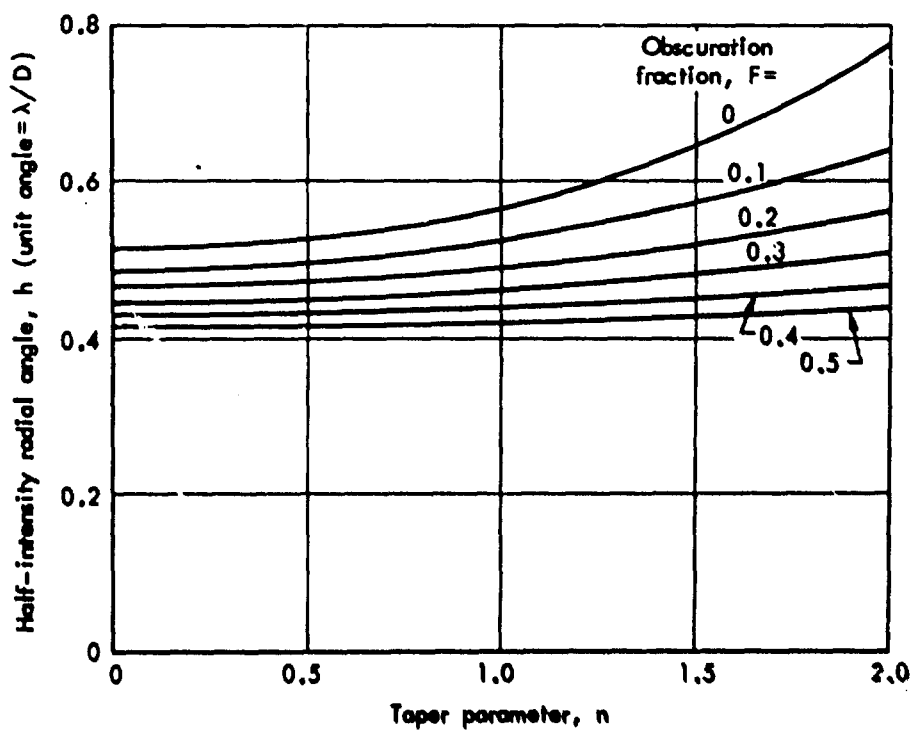


Fig. 10—Half-intensity radial angles

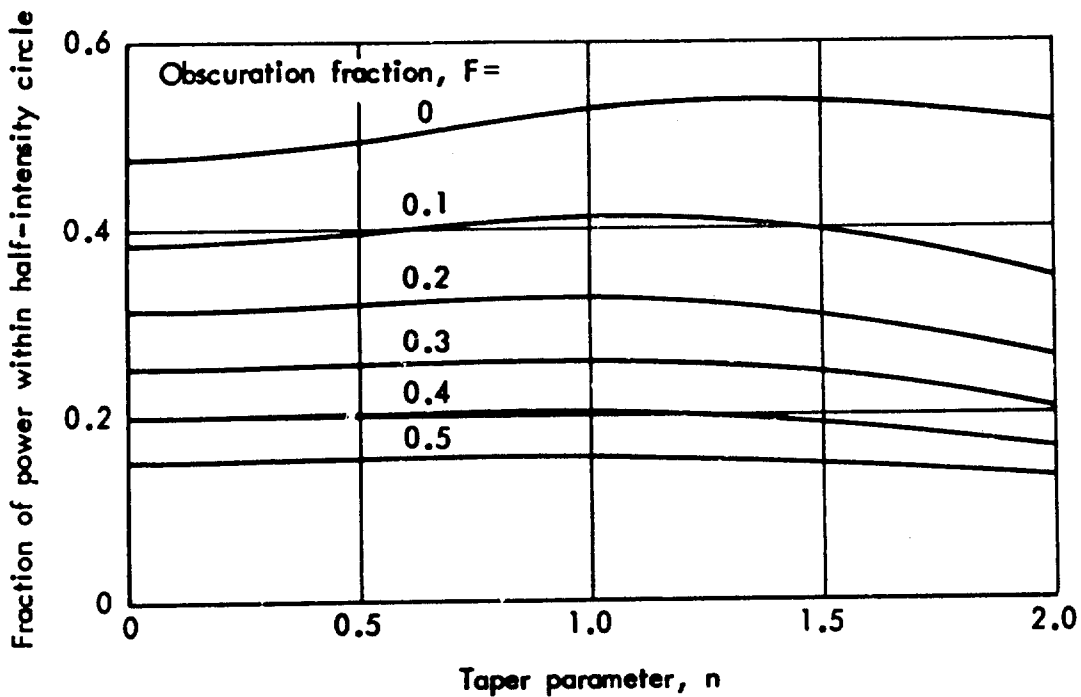


Fig. 11—Fraction of image power within half-intensity circle

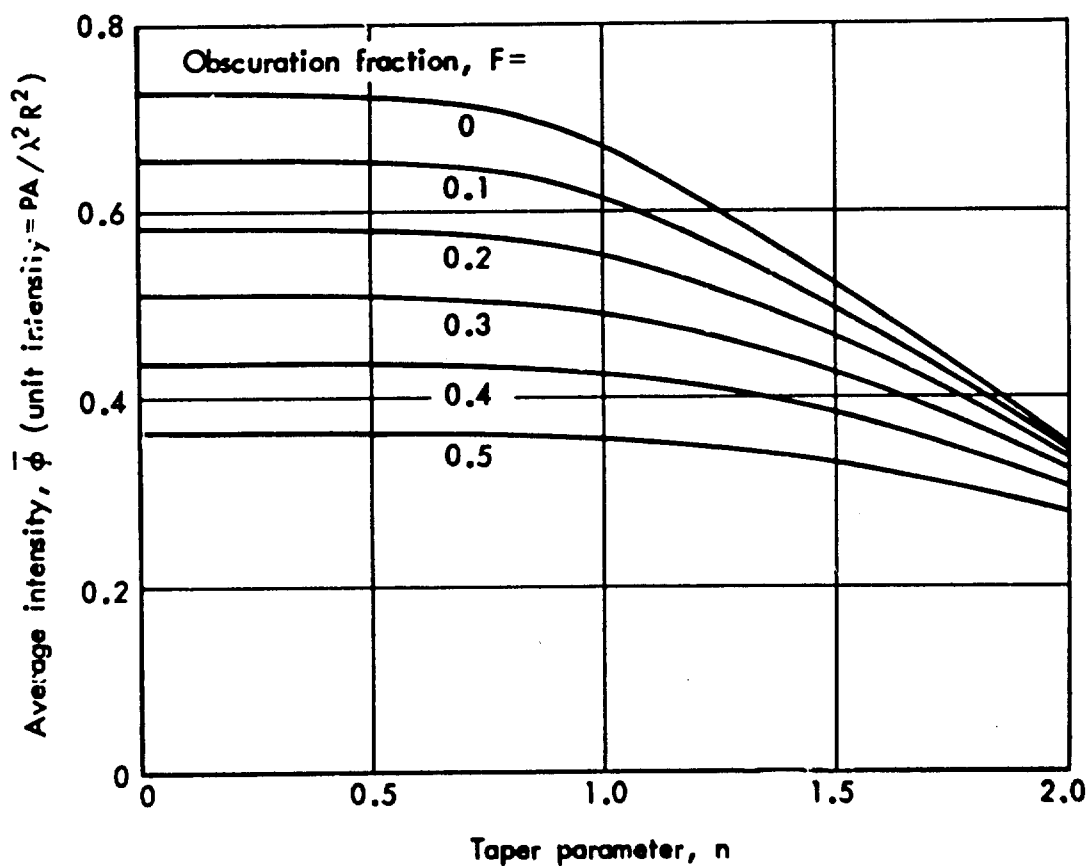


Fig. 12—Average intensity within half-intensity circle

Table 5; ϕ_o from Table 2) for each of the pairs of values for n and F and found that

$$0.724 \leq \frac{\bar{\phi}}{\phi_o} \leq 0.729 \quad (12)$$

Therefore, the relationship $\bar{\phi} = 0.727 \phi_o$, which is correct for the Airy pattern ($n = 0$, $F = 0$), remains correct within 0.5 percent over the entire range of tapers and obscuration considered in this study--a very broad range.

Apparently, the central portions of these diffraction patterns--out to the half-intensity circle at least--have a characteristic shape. That is, one curve of ϕ versus β can probably be transformed very nearly into any of the others simply by changing scales.

The plausibility of this result is indicated by the following argument.* The Bessel function $J_o(x)$ can be expressed as a power series that has the form $J_o(x) = 1 - a_2 x^2 + a_4 x^4 - a_6 x^6 + \dots$, where the a 's are known constants. If $J_o(\pi\beta z)$ in the diffraction integral (Eq. (5)) were replaced by its series and the term-by-term integration completed, the resultant expression for the amplitude $U(\beta)$ would have the form $U(\beta) = b_0 - b_2 \beta^2 + b_4 \beta^4 - b_6 \beta^6 + \dots$, where the b 's are constants. In the region of interest, β remains small; therefore, the first two terms may dominate the series. Assuming this to be true, it is easy to show that if $U(\beta) = b_0 - b_2 \beta^2$, then $\bar{\phi}/\phi_o = 0.736$, independent of the values of b_0 and b_2 .

Estimates for the $1/e^2$ Disc

In light of the pattern consistencies described above, it seems plausible that reasonably constant relationships exist between characteristics of the $1/e^2$ disc and the half-intensity disc. To test this conjecture, we can manipulate the results presented in Table 1, which shows characteristics of both discs for four different sets of aperture

* Developed by W. Sollfrey, of The Rand Corporation.

conditions. For each set of aperture conditions, the ratios of results for the $1/e^2$ disc to results for the half-intensity disc fall within the following narrow boundaries:

$$K_1 = \text{ratio of angular radii} = 1.60 \pm 0.02$$

$$K_2 = \text{ratio of power fractions} = 1.62 \pm 0.02$$

$$K_3 = \text{ratio of average intensities} = 0.630 \pm 0.007$$

Consequently, the ratios do appear to be reasonably constant (but the agreement between K_1 and K_2 is probably a coincidence). Therefore, if the $1/e^2$ disc is used as the spot, its characteristics can be estimated from the following:

$$\text{Angular radius} = 1.6 h \quad (13)$$

$$\text{Power fraction} = 1.6 f \quad (14)$$

$$\text{Average intensity} = 0.63 \bar{\phi} \quad (15)$$

where h , f , and $\bar{\phi}$ are the values for the half-intensity disc.

III. ENERGY DENSITIES PRODUCED BY A JITTERING BEAM

For most laser applications, it is necessary to know how much energy will be delivered to certain areas of the target when the laser operates for a time interval t . If the diffraction pattern stays fixed with respect to the target plane, the calculation is straightforward. The appropriate intensities can be estimated by the methods described earlier and then multiplied by t to get energies. However, if the pattern moves laterally, the intensities at fixed points on the target plane do not stay constant during t . This could complicate the energy calculations by requiring integrations rather than simple multiplications.

In some situations, random processes may cause the center of the pattern to "jitter" about an aim point during the time interval t . The problem of estimating the energy delivered by a jittering beam is simplified if the time-averaged intensity at a point can be treated as being reasonably independent of the value of t . It is further simplified if circular gaussian functions can be used to describe both the beam motion and the beam shape.

A METHOD FOR ESTIMATING THE TIME-AVERAGED INTENSITY

Let the aim point be the origin of a rectangular coordinate system in the target plane. Let (x, y) denote the locations of the beam center at randomly chosen instants. We postulate that x and y are independent and are normally distributed with zero means and identical standard deviations σ_J . The probability that the beam center will be located within a small area $dx dy$ surrounding a particular point (x, y) is thus given by $\psi(x, y) dx dy$, where $\psi(x, y)$ is the product of two normal probability density functions (pdf); i.e.,

$$\psi(x, y) = \frac{1}{\sqrt{2\pi \sigma_J}} e^{-x^2/2\sigma_J^2} \cdot \frac{1}{\sqrt{2\pi \sigma_J}} e^{-y^2/2\sigma_J^2}$$

or more simply,

$$\psi(\rho) = \frac{1}{2\pi\sigma_J^2} e^{-\rho^2/2\sigma_J^2} \quad (16)$$

where $\rho^2 = x^2 + y^2$. The function $\psi(\rho)$ is called the circular gaussian pdf. For want of a better term, σ_J is often called the "standard deviation" of the circular distribution, even though it is not the standard deviation of ρ .

It was shown in Eqs. (2) and (3) that for a gaussian beam, the intensity $I(q)$ at a radial distance q from the axis of the beam can be expressed in the form

$$I(q) = I_0 e^{-2q^2/w_0^2}$$

where $I_0 = 2 P/\pi w_0^2$, and w_0 is the beam "radius" at the focus. For consistency of notation, it is advantageous to introduce a beam "standard deviation" by the substitution $\sigma_D = w_0/2$. The resulting expression for $I(q)$ is

$$I(q) = \frac{P}{2\pi\sigma_D^2} e^{-q^2/2\sigma_D^2} \quad (17)$$

which is identical in form to a circular gaussian pdf except for the inclusion of the power P .

As the beam moves, the intensity at a fixed point (x_0, y_0) will vary. When the center of the beam is at a point (x, y) the intensity at (x_0, y_0) is

$$I(x_0, y_0, x, y) = \frac{P}{2\pi\sigma_D^2} \exp \left\{ -\frac{(x_0 - x)^2 + (y_0 - y)^2}{2\sigma_D^2} \right\}$$

To find the expected-value or "average" intensity $\overline{I(x_0, y_0)}$ at the point (x_0, y_0) we must evaluate the integral

$$\overline{I(x_0, y_0)} = \iint_{-\infty}^{\infty} I(x_0, y_0, x, y) \cdot \psi(x, y) dx dy$$

In Ref. 12 it is shown that this integral yields the result

$$\overline{I(x_0, y_0)} = \frac{P}{2\pi(\sigma_D^2 + \sigma_J^2)} e^{-\rho_0^2/2(\sigma_D^2 + \sigma_J^2)} \quad (18)$$

where $\rho_0^2 = x_0^2 + y_0^2$. This is another gaussian distribution. It indicates that the formula for the average intensities has the same mathematical form as it would have if the gaussian diffraction pattern had been held stationary but broadened so that its "standard deviation" became $\sqrt{\sigma_D^2 + \sigma_J^2}$. This is a most useful result for two reasons: (1) The energy calculations reduce again to simple multiplications by t , and (2) gaussian functions are usually easy to manipulate. For example, for a gaussian intensity distribution with total power P and standard deviation σ , it is straightforward to show that the maximum intensity is $I_0 = P/2\pi\sigma^2$, the radius of the $1/e^2$ disc is 2σ , the power within it is 0.865 P , and its average intensity is $0.432 I_0$.⁽¹²⁾ For the half-intensity disc, the corresponding quantities are: radius = 1.177σ , contained power = 0.5 P , and average intensity = $0.721 I_0$.

THE GAUSSIAN APPROXIMATION

To use the simplified treatment of jitter described above, we must approximate a real diffraction pattern with a gaussian pattern.* Clearly, the central portions where the high intensities occur are the regions we should try to match most closely. It follows that a "good" gaussian

* "Real" means only that a pattern has been computed from a diffraction integral.

approximation will not necessarily represent the delivery of the same total power as is contained in the real pattern. Therefore, we will reserve the symbol P for the real total power and define a "gaussian power-correction factor" G such that GP is the total power in the gaussian image. The formula for the gaussian intensity pattern then becomes

$$I(\rho) = \frac{GP}{2\pi\sigma_D^2} e^{-\rho^2/2\sigma_D^2} \quad (19)$$

A more convenient form for this equation can be achieved by introducing the same kinds of dimensionless quantities as were used in Section II. The variable β and a "dimensionless standard deviation" s are introduced by using the relationships $\rho = \beta(\lambda/D)R$ and $\sigma_D = s(\lambda/D)R$.

The resulting formula for the intensity is

$$I(\beta) = \frac{PA}{\lambda^2 R^2} \cdot \frac{2G}{\pi^2 s^2} e^{-\beta^2/2s^2} \quad (20)$$

Then, by again choosing the unit of intensity to be $PA/\lambda^2 R^2$, we obtain the dimensionless gaussian intensity distribution $\phi(\beta)$

$$\phi(\beta) = \frac{2G}{\pi^2 s^2} e^{-\beta^2/2s^2} \quad (21)$$

In this formulation, all of the characteristics of the gaussian pattern are determined by the values of the two independent parameters s and G . By choosing an appropriate pair of values for these parameters, we can match at least two of the characteristics of a real pattern.

Methods for Selecting s and G

Section II presented characteristics of real diffraction patterns

that result from various tapers and obscurations. In that discussion, we emphasized the maximum intensity ϕ_0 and three characteristics of the half-intensity disc: the radial angle h , the power fraction f , and the average intensity $\bar{\phi}$. Also it was noted that the three half-intensity quantities are not independent because of the relationship $\bar{\phi} = 4f/\pi h^2$. Consequently, ϕ_0 , h , f , and $\bar{\phi}$ represent only three independent characteristics.

A gaussian approximation can fit two of these three independent characteristics. The method consists of first using Eq. (21) to express ϕ_0 , h , f , and $\bar{\phi}$ for a gaussian in terms of s and G . The maximum intensity ϕ_0 is

$$\phi_0 = \frac{2G}{\pi^2 s^2} \quad (22)$$

To find the half-intensity radial angle h , we set $\exp(-h^2/2s^2) = \frac{1}{2}$ and obtain

$$h = s \cdot \sqrt{\ln 4} = 1.177 s \quad (23)$$

The fraction f of the real image power P within the half-intensity circle is

$$f = \frac{\pi^2}{2} \int_0^h \phi(\theta) \theta d\theta$$

$$= G(1 - e^{-h^2/2s^2}) + \frac{1}{2} G \quad (24)$$

Finally, the average intensity $\bar{\phi}$ is

$$\bar{\phi} = \frac{4f}{\pi h^2} \quad (25)$$

or

$$\bar{\phi} = \frac{2G}{\pi^2 s^2 \ln 4} = 0.721 \frac{2G}{\pi^2 s^2} \quad (26)$$

The above relationships can be used in reverse to select s and G when ϕ_0 , h , f , and $\bar{\phi}$ are given for a real pattern. To make the gaussian pattern have the same half-intensity radius h as the real pattern, we set

$$s = \frac{h}{1.177} \quad (27)$$

The parameter G can then be chosen so that either ϕ_0 or $\bar{\phi}$ is matched. To match the peak intensity,

$$G = \frac{\pi^2 s^2}{2} \phi_0 \quad (28)$$

If we wish to match the average intensity $\bar{\phi}$, the proper formula for G is either

$$G = \frac{\pi^2 s^2 \ln 4}{2} \bar{\phi} \quad (29)$$

or

$$G = 2f \quad (30)$$

whichever is more convenient.

A Numerical Example and Recommended Method

Consider the diffraction pattern that results from the aperture conditions $n = 1$ and $F = 0.1$. (This is a gaussian illumination with $1/e^2$ truncation and 10 percent obscuration, which was examined in detail in Section II.) From Table 1 (or Tables 2 through 5), we find $\phi_0 = 0.844$, $h = 0.522$, $f = 0.412$, and $\bar{\phi} = 0.613$.

We approximate it with a gaussian that has the correct radius and average intensity for the half-intensity disc; i.e.,

$$s = \frac{h}{1.177} = 0.444$$

$$C = 2f = 0.824$$

For these values the equation for the gaussian intensity distribution (Eq. (21)) becomes

$$\phi(\beta) = 0.847 e^{-\beta^2/0.394} \quad (31)$$

and the resultant fraction $f(\beta)$ of the real image power P that is within a circle of radius β can easily be shown to be

$$\begin{aligned} f(\beta) &= G(1 - e^{-\beta^2/2s^2}) \\ &= 0.824 (1 - e^{-\beta^2/0.394}) \end{aligned} \quad (32)$$

In Figs. 13 and 14 the intensities and the power fractions of the approximation are compared with those of the real diffraction pattern. This comparison shows that the gaussian function is an excellent approximation for the central, high-intensity portions of the pattern.

Note that although we made no explicit attempt to match the peak value ϕ_0 , a nearly perfect match occurred (0.844 for the real pattern; 0.847 for the gaussian pattern). This agreement is not a coincidence, and it is not limited to the specific example chosen here. In Section II (Eq. (12)), it was found that for real diffraction patterns, the relationship $\bar{\phi} = 0.727 \phi_0$ remains correct to within about 0.5 percent. For a gaussian pattern, it is easily seen from Eqs. (22) and (26) that $\bar{\phi}_0 = 0.721 \phi_0$. These two equations are similar enough that it makes little difference whether the gaussian is fitted to $\bar{\phi}$ or ϕ .

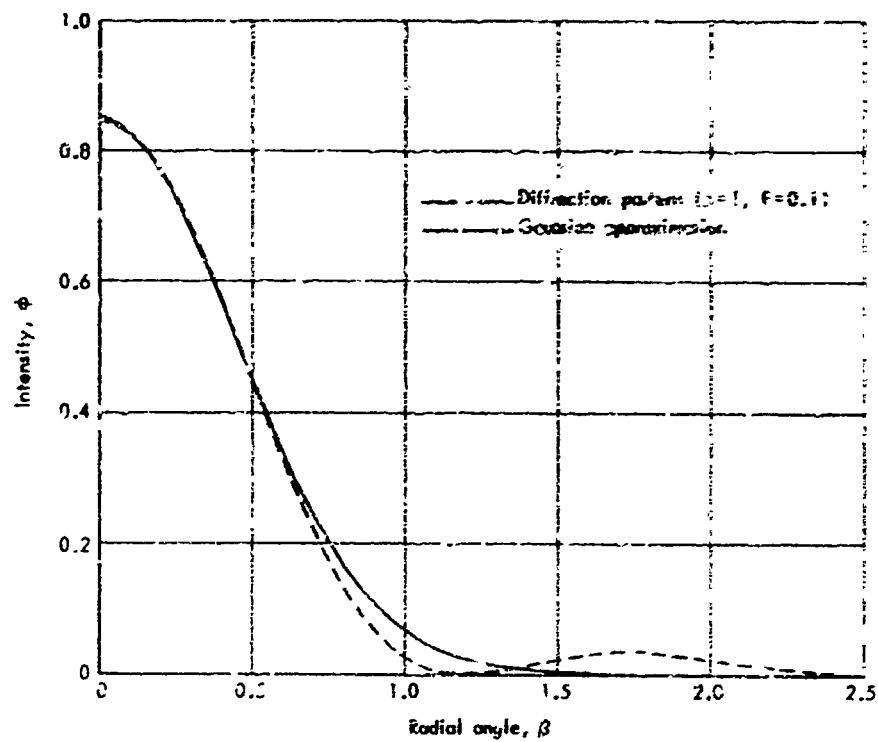


Fig. 13—Comparison of intensities

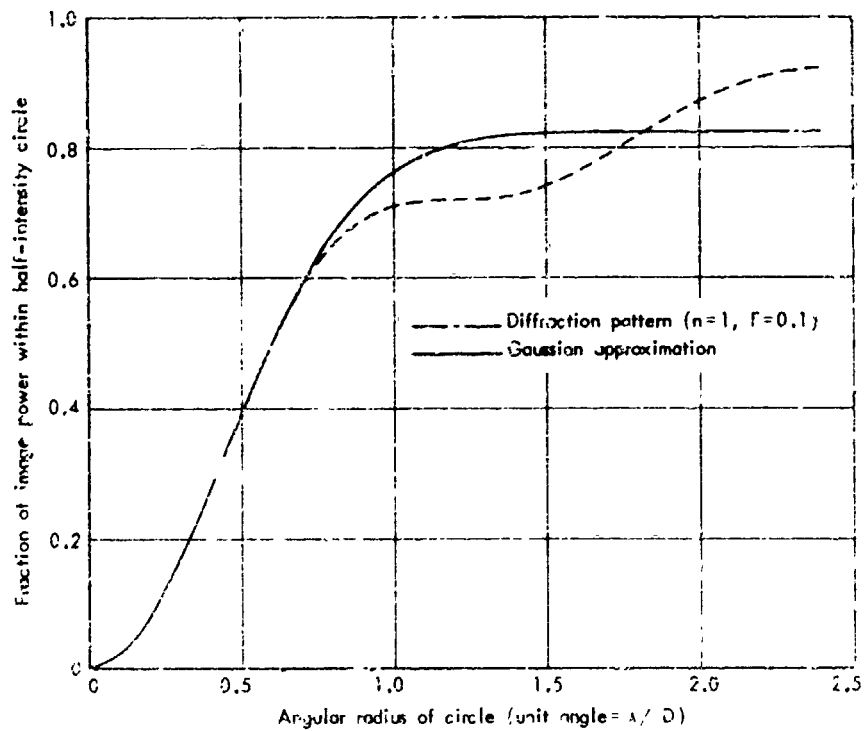


Fig. 14—Comparison of power fractions

The simplest approach appears to be the one adopted for this example. Namely, choose s and G so that the gaussian pattern and the real pattern yield the same radius and average intensity for the half-intensity disc. The formulas are

$$s = \frac{h}{\sqrt{\ln 4}} = \frac{h}{1.177}$$

$$G = 2f$$

where h and f are as given in Section II.

Comments on a Special Case

An aperture illumination that is often chosen as "representative" is an unobscured gaussian with $1/e^2$ truncation ($n = 1$, $F = 0$). The resultant diffraction-pattern characteristics for this case are presented in the third column of Table 1 in Section II.

Suppose we wish to approximate this pattern with a gaussian that matches the $1/e^2$ disc rather than the half-intensity disc. From Table 1, the disc radius ($2s$) is 0.915, so we let $s = 0.915/2 = 0.458$. The power fraction, from Table 1, is 0.866. By coincidence, this is almost exactly the correct value for a gaussian (0.865), and therefore, no power correction is needed ($G = 1$). Consequently, a gaussian distribution with a total power P and a standard deviation of $\sigma_D = 0.458 \frac{\lambda}{D} R$ will match the radius and the average intensity of the $1/e^2$ disc of the real pattern.

Now consider a totally different derivation of a gaussian pattern. An approximation that has sometimes appeared in the literature results from matching P and choosing σ_D so that the gaussian has the same maximum intensity as that of the ideal Airy pattern. Equating the two maxima gives

$$\frac{P}{2\pi\sigma_D^2} = \frac{\pi}{4} \frac{P D^2}{\lambda^2 R^2}$$

which yields

$$\sigma_D = \frac{\sqrt{2}}{\pi} \frac{\lambda}{D} R \quad (33a)$$

$$= 0.450 \frac{\lambda}{D} R \quad (33b)$$

which, by another coincidence, is very close to the value of σ_D derived from Table 1.

These coincidences help to explain and to justify equations developed by Peckham in Ref. 12. In that report he postulates the same aperture illumination: gaussian with $1/e^2$ truncation. He then introduces Eq. (33a), attributes it to Buck (Ref. 13), and states that it predicts the $1/e^2$ radius of the real diffraction pattern. Finally, he conjectures that a gaussian with the same $1/e^2$ radius (and the same power) will be an adequate approximation to the real image.*

The analyses presented here show that a gaussian with the same power and $1/e^2$ radius as the real image would also have the same average intensity over the $1/e^2$ disc. Therefore, they support Peckham's conjecture that this approximation is adequate (for this particular aperture illumination).

The method recommended in the present report produces a slightly different approximation. The power in the gaussian becomes 1.06 P and the standard deviation increases to $\sigma_D = 0.481 \frac{\lambda}{D} R$. The high-intensity portion of the pattern is fitted more closely, but it seems doubtful that these differences would prove to be important.

FINAL FORM OF THE INTENSITY EQUATION

For the gaussian intensity distribution that results from a jittering beam, the average physical intensity over the spot is kI_o , where I_o is the maximum intensity and k is a constant that depends only on the

* In subsequent personal communications, Peckham explained that he was aware of Eq. (33a) and discovered that it was consistent with numerical results presented graphically by Buck, but he was unaware of its derivation.

definition of spot size. As noted earlier, $k = 0.432$ for the $1/e^2$ disc and 0.721 for the half-intensity disc. Here we need only discuss I_o .

From Eq. (18), but with P replaced by GP , the proper formula for I_o is

$$I_o = \frac{GP}{2\pi(\sigma_D^2 + \sigma_J^2)}$$

In this formulation, σ_D and σ_J have the dimensions of length. Since jitter and the beamspread are usually treated as angles viewed from the aperture, we introduce the angular standard deviations α_D and α_J to get

$$I_o = \frac{GP}{2\pi R^2(\alpha_D^2 + \alpha_J^2)} \quad (34)$$

and since $\alpha_D = s \frac{\lambda}{D}$, the equation becomes

$$I_o = \frac{GP}{2\pi R^2[(s \frac{\lambda}{D})^2 + \alpha_J^2]} \quad (35)$$

This is a basic equation for the intensity. It explicitly contains the parameters G and s that are chosen to fit the nonjittering pattern with a gaussian. However, one alteration is needed to allow the analyst to introduce a degradation in beam quality: The methods used to obtain the results presented in Section II imply that the beam is "diffraction-limited." In Ref. 12 an "m times diffraction-limited" beam is defined as one for which the standard deviation of the beam is increased from α_D to $m\alpha_D$. Thus, introduction of this parameter gives the final form of the intensity equation,

$$I_o = \frac{GP}{2\pi R^2[m^2(s \frac{\lambda}{D})^2 + \alpha_J^2]} \quad (36)$$

This equation is similar in form to one developed by Peckham⁽¹²⁾ and used by Davis⁽¹⁴⁾ to study the relative advantages of laser systems that produce different wavelengths.

Equation (36) can be written in many different ways, some of which might not be immediately recognizable as the same equation. For example, R. O. Hundley of Rand, in several publications prepared for ARPA, expresses the intensity as an ideal value multiplied by a degradation factor that accounts for jitter (and degradation associated with atmospheric effects). To convert to Hundley's equation, we let $m = 1$ and rewrite $I = k I_0$ as

$$I = K \frac{PD^2}{\lambda^2 R^2} \cdot \frac{1}{\left[1 + \left(\frac{\alpha_J}{\alpha_D} \right)^2 \right]}$$

where $K = kG/2\pi s^2$. The term $KPD^2/\lambda^2 R^2$ is the undegraded intensity. If I is to be the average intensity within the half-intensity circle, then K is simply $\bar{\phi} \pi/4$, where $\bar{\phi}$ is found from Section II. One other change is needed to complete the conversion. As long as the correct value for the ratio α_J/α_D is maintained, other measures of the jitter statistics or beam dimensions can be used. Hundley uses θ_J , the angular diameter of the circle that contains the beam center 50 percent of the time, and θ_D , the angular diameter of the half-intensity circle. These are consistent parameters. He notes that $\theta_D \approx \lambda/D$ for a wide range of aperture conditions (this corresponds to $h \approx 0.5$)^{*} and uses $\theta_J/(\lambda/D)$ for the appropriate ratio. The resulting equation is

$$I = K \frac{PD^2}{\lambda^2 R^2} \cdot \frac{1}{\left[1 + \frac{\theta_J^2}{(\lambda/D)^2} \right]}$$

^{*}See Fig. 10.

REFERENCES

1. Boyd, G. D., and J. P. Gordon, "Confocal Multimode Resonator for Millimeter Through Optical Wavelength Masers," *Bell System Technical Journal*, Vol. 40, March 1961, p. 489.
2. Kogelnik, H., and T. Li, "Laser Beams and Resonators," *Proceedings of the IEEE*, Vol. 54, No. 1, October 1966, p. 1312.
3. Dickson, L. D., "Characteristics of a Propagating Gaussian Beam," *Applied Optics*, Vol. 9, No. 8, August 1970, p. 1854.
4. Bloom, Arnold L., *Gas Lasers*, John Wiley & Sons, Inc., New York, 1968, p. 114.
5. Born, Max, and Emil Wolf, *Principles of Optics*, Third (Revised) Edition, Chapter VIII, Pergamon Press, New York, 1965.
6. Campbell, J. P., and L. G. DeShazer, "Near Fields of Truncated-Gaussian Apertures," *Journal of the Optical Society of America*, Vol. 59, No. 11, November 1969, p. 1427.
7. Schell, Richard G., and George Tyras, "Irradiance from an Aperture with a Truncated-Gaussian Field Distribution," *Journal of the Optical Society of America*, Vol. 61, No. 1, January 1971, p. 31.
8. Barakat, Richard, "Solution of the Luneberg Apodization Problems," *Journal of the Optical Society of America*, Vol. 52, No. 3, March 1962, p. 264.
9. Holmes, D. A., P. V. Avizonis, and K. H. Wrolstad, "On-Axis Irradiance of a Focused, Apertured Gaussian Beam," *Applied Optics*, Vol. 9, No. 9, September 1970, p. 2179.
10. Olaofe, G. Oluremi, "Diffraction by Gaussian Apertures," *Journal of the Optical Society of America*, Vol. 60, No. 12, December 1970, p. 1654.
11. Gerry, Edward T., "Gasdynamic Lasers," *IEEE Spectrum*, November 1970, p. 51.
12. Peckham, Lawrence N., *A Simplified Equation for Calculating Far-Field Intensity*, Technical Report No. AFWL-TR-71-39, Air Force Weapons Laboratory, Kirtland Air Force Base, New Mexico, April 1971.
13. Buck, Arden L., "The Radiation Pattern of a Truncated Gaussian Aperture Distribution," *Proceedings of the IEEE*, March 1967, p. 448.

Preceding page blank

14. Davis, Richard W., *The Effect of Wavelength and Jitter on Far-Field Intensity*, Technical Note No. AFWL-TN-LEAPS-001, Air Force Weapons Laboratory, Kirtland Air Force Base, New Mexico, July 1971.
15. Lutomirski, R. F., *Propagation of a Focused Laser Beam in a Turbulent Atmosphere*, The Rand Corporation, R-608-ARPA, June 1971.